

University of Wollongong

Research Online

Faculty of Engineering and Information
Sciences - Papers: Part A

Faculty of Engineering and Information
Sciences

1-1-2014

A tool-path generation strategy for wire and arc additive manufacturing

Donghong Ding

University of Wollongong, dd443@uowmail.edu.au

Zengxi Stephen Pan

University of Wollongong, zengxi@uow.edu.au

Dominic Cuiuri

University of Wollongong, dominic@uow.edu.au

Huijun Li

University of Wollongong, huijun@uow.edu.au

Follow this and additional works at: <https://ro.uow.edu.au/eispapers>



Part of the [Engineering Commons](#), and the [Science and Technology Studies Commons](#)

Recommended Citation

Ding, Donghong; Pan, Zengxi Stephen; Cuiuri, Dominic; and Li, Huijun, "A tool-path generation strategy for wire and arc additive manufacturing" (2014). *Faculty of Engineering and Information Sciences - Papers: Part A*. 2729.

<https://ro.uow.edu.au/eispapers/2729>

Research Online is the open access institutional repository for the University of Wollongong. For further information contact the UOW Library: research-pubs@uow.edu.au

A tool-path generation strategy for wire and arc additive manufacturing

Abstract

This paper presents an algorithm to automatically generate optimal tool-paths for the wire and arc additive manufacturing (WAAM) process for a large class of geometries. The algorithm firstly decomposes 2D geometries into a set of convex polygons based on a divide-and-conquer strategy. Then, for each convex polygon, an optimal scan direction is identified and a continuous tool-path is generated using a combination of zigzag and contour pattern strategies. Finally, all individual sub-paths are connected to form a closed curve. This tool-path generation strategy fulfils the design requirements of WAAM, including simple implementation, a minimized number of starting-stopping points, and high surface accuracy. Compared with the existing hybrid method, the proposed path planning strategy shows better surface accuracy through experiments on a general 3D component.

Keywords

wire, path, arc, tool, additive, manufacturing, generation, strategy

Disciplines

Engineering | Science and Technology Studies

Publication Details

Ding, D., Pan, Z., Cuiuri, D. & Li, H. (2014). A tool-path generation strategy for wire and arc additive manufacturing. *International Journal of Advanced Manufacturing Technology*, 73 (1-4), 173-183.

A tool-path generation strategy for wire and arc additive manufacturing

Donghong Ding, Zengxi (Stephen) Pan, Dominic Cuiuri, Huijun Li

School of Mechatronics, Faculty of Engineering and Information Sciences, University of Wollongong, Northfield Ave, Wollongong, NSW 2500, Australia

Abstract: This paper presents an algorithm to automatically generate optimal tool-paths for the wire and arc additive manufacturing (WAAM) process for a large class of geometries. The algorithm firstly decomposes 2D geometries into a set of convex polygons based on a divide-and-conquer strategy. Then, for each convex polygon, an optimal scan direction is identified and a continuous tool-path is generated using a combination of zigzag and contour pattern strategies. Finally, all individual sub-paths are connected to form a closed curve. This tool-path generation strategy fulfils the design requirements of WAAM, including simple implementation, a minimised number of starting-stopping points, and high surface accuracy. Compared with the existing hybrid method, the proposed path planning strategy shows better surface accuracy through experiments on a general 3D component.

Keywords: arc welding, tool-path generation, geometry decomposition, additive manufacturing

1 Introduction

Additive manufacturing (AM) machines have evolved over the last three decades from a limited number of expensive prototypes to widely available small-scale commodity production tools [1]. These machines can automatically fabricate arbitrarily shaped parts layer-by-layer from almost any material. The AM process has drawn significant research interest for a variety of industrial applications in the manufacturing, medical, architecture, aerospace, and automotive sectors. A particularly interesting application is the production of large sized aerospace components that are currently machined from costly wrought material, such as Ti-6Al-4V. AM offers the possibility of producing these parts at very low fly-to-buy ratios in comparison to current production practices.

Many techniques have been developed for manufacturing metal structures in AM, such as Selective Laser Sintering [2], Direct Metal Deposition [3], Electron Beam Freeform Fabrication [4], Shape Deposition Manufacturing [5], and WAAM [6-8], etc. In terms of power sources, AM can be classified into three groups, namely, laser, electron, and arc. WAAM is by definition an arc-based process that uses either the Gas Tungsten Arc Welding (GTAW) or the Gas Metal Arc Welding (GMAW) process, and is considered to be a promising technology for fabricating functional metal parts. With the advantages of higher deposition rate, lower costs, and safer operations, WAAM is considered to be a more realistic

method for manufacturing aerospace components with median to large size. Generally, the deposition rate of laser or electron beam deposition is in the order of 2-10 g/min, compared to 50-130 g/min for WAAM [9].

However, a mature WAAM system is still not commercially available to industry at present due to a number of inherent technical challenges, such as distortion and residual stress from excessive heat input, and uneven weld bead geometry distribution within weld paths. The issue of distortion and residual stress could be minimized through using thermal tensioning technology or adopting a low heat input process such as Cold Metal Transfer (CMT), but these issues are beyond the scope of this paper. This paper focuses on improving the weld bead geometry and increasing the surface accuracy of the built parts through improved tool-path planning. Uneven weld bead geometry may lead to the accumulation of errors in the vertical direction after the deposition of several layers. Figure 1 shows an example of thin walls built by weld deposition where there are significant differences in bead geometry at the start and end of the weld paths [10]. As can be seen, the errors introduced in lower layers are compounded as further layers are added. To overcome the issue of uneven surface induced by arc start and arc end procedures, Zhang et al. [11] adjusted the deposition parameters at the start and end portions of weld paths to flexibly control the weld bead geometry. However, the control procedures are empirical and time-consuming. Hybrid layer manufacturing processes, which combine the means of both additive and subtractive manufacturing, have recently been developed [12, 13]. The hybrid processes employ intermediate machining of the upper surface between successive layer depositions to overcome the layer surface roughness and to avoid the cumulative deviations in build height. Nevertheless, such cleaning steps increase the complexity of the system, and reduce the productivity of AM technology.



Fig.1 Thin walls built by weld deposition showing the changing bead geometry at the start and end of weld paths [10]

This paper develops a path planning algorithm to improve surface accuracy of the WAAM process. The proposed path planning algorithm is able to generate a continuous tool-path to fill a large class of geometries without starting-stopping sequences. The current state of research on path generation strategy is reviewed in Section 2. Section 3 introduces the detailed path planning algorithms. Section 4 presents the implementation of the algorithm and experimental results, followed by a conclusion in Section 5.

2 Literature review

Many types of tool-path patterns have been developed for AM processes in general, as shown in Table 1. For any 3 dimensional component to be fabricated, the object is sliced into a number of 2D layers of defined thickness. Each layer of deposition may consist of a number

of tool-path passes. Each tool-path pass is defined as a continuous deposition of materials with a single start and stop. Each tool-path pass may consist a few tool-path elements, which are straight-line sections. Examples are raster, zigzag, contours, space filling curves, and hybrid tool-path planning approaches.

Table 1. Summary of AM tool-path generation methods.

References	Tool path strategy	Advantages	Disadvantages
[14]	Raster	+ a	- b, - c, - d
[15, 16]	Zigzag	+ a	- b, - c, - d
[17-19]	Contour	+ b	- a, - c
[20, 21]	Spiral	+ c	- a
[22, 23]	Fractal space curves	+ c	- a, - d
[22, 24, 25]	Continuous	+ c	- a, - d
[11, 26]	Hybrid	+ a, + b	- c, - d

Major performance indicators of tool-path generation methods	
a	Easy implementation & Simple algorithms
b	Good geometrical accuracy
c	Less tool-path passes
d	Less tool-path elements

The raster scanning path technique is based on planar ray casting along one direction [14]. In this strategy, 2D regions are filled by a set of scan lines with finite width. It is commonly employed in commercial AM systems due to its simple implementation and suitability for almost any arbitrary boundary.

Derived from the raster strategy, zigzag tool-path generation is the most popular method used in commercial AM systems. While it fills geometries line-by-line along one direction like the raster approach, the zigzag approach combines the separate parallel lines into a single continuous pass which significantly reduces the number of tool-path passes [15, 16]. This method significantly improves the productivity of the AM process by reducing the required transition motions of the machine. However, the outline accuracy of the part for both raster and zigzag approaches is poor due to the discretization errors on any edge that is not parallel to the tool motion direction.

Contour path generation, which is another typical method, can address the above geometrical quality issue effectively by following the geometrical trend of the boundary contours [17, 18]. Various contour-map patterns were investigated by Li et al. [19] to develop optimal tool-path patterns for sculptured parts with a single island and no seriously non-convex shape. However, by offsetting the contours, the scheme generates numerous closed curves which are disconnected and therefore not suitable for WAAM.

The spiral tool-path generation has been widely applied in numerically controlled (NC) machining, especially for 2D pocket milling and uniform pocket cutting [20, 21]. This method can also be used to solve the problems of zigzag tool-paths in AM process, but is only suitable for certain special geometrical models [22].

Another tool-path planning method is based on fractal space filling curves. Bertoldi et al. [23] applied Hilbert curve-based tool-paths to the Fused Deposition Modelling process. It has been found to be particularly useful in reducing shrinkage during AM fabrication processes. However, the large number of path direction turning motions that are produced by using this

strategy are not suitable for WAAM. Chiu et al. [24] proposed a methodology to realize the fabrication of a fractal represented model by AM. In the proposed methodology, a slab grid that consists of a number of pixels in each layer is first generated, and then checked so that slab models of the fractal are created. Finally the boundary of the slab model is refined and the tool-path of the object can be generated from these boundaries. This methodology provides the possibility of fabricating a fractal prototype, but it is not suitable for conventional engineering parts.

Continuous path planning can be considered as another tool-path generation method. Hilbert filling curve applied by Bertoldi et al. [23] is a continuous path, which can cover a region of space without intersecting itself. Wasser et al. [25] introduced a fractal-like build style using a simulated annealing algorithm. This method is able to generate filling patterns that allow the continuous deposition of a single path to fill arbitrarily shaped area. In this method, the area to be deposited is firstly decomposed into nodes, with the number of the nodes determined by the accuracy requirement of the AM process. However, when the area to be filled is large and the accuracy requirement is high, the processing time required would be unacceptably long. Moreover, highly convoluted paths may result in accumulation of heat in certain regions, therefore inducing excessive distortion of the part. Frequent alternations of tool-path travel directions are also not preferred in WAAM. Dwivedi et al. [26] developed a continuous path planning approach for AM. In this method, the 2D geometry is firstly decomposed into a set of monotone polygons. For each monotone polygon, a closed zigzag curve is then generated. Finally, a set of closed zigzag curves are combined together into an integrated continuous torch path. The continuous path planning approach significantly reduces the number of welding passes. However, purely employing zigzag based curves would have a surface accuracy issue, as Zhang et al. [11] point out the importance of filling the outline of the image with vector motions in WAAM.

The hybrid path planning strategy is promising as it shares some merits of various approaches. A combination of contour and zigzag pattern is commonly developed to meet both the geometrical accuracy and build efficiency requirements. Zhang et al. [11] developed a new image algorithm for welding-based AM. The planned approach includes one inner zigzag path which is faster and more universal, and one outline vector path which is very helpful for maintaining the surface accuracy and quality. Jin et al. [27] proposed a mixed tool-path algorithm to generate contour and zigzag tool-path for AM of biomedical models. The zigzag tool-path is employed to fill the interior area of the part to improve the efficiency, while the contour tool-path is used to fabricate the area along the boundary of the contours to improve the geometrical quality of the model.

Compared to most of the existing path planning techniques that are designed for AM processes using a laser heat source, the path planning generation for WAAM has unique requirements due to the inherent features of the arc welding deposition system. Requirements of a tool-path planning strategy for WAAM are summarised as follows:

1. Geometrical accuracy: as the resolution of arc welding is relatively low, the outlines of 2D geometries should be fabricated by contour patterns which could effectively improve the geometrical quality of the part.
2. Minimize the number of tool-path passes: the cumulative deviations introduced by the uneven weld bead geometry at the start and end portions of each welding pass will

limit the maximum number of layers that can be added together before vertical build errors become problematic. Therefore, the number of welding passes should be minimized to reduce starting-stopping sequences within each layer. A continuous path is preferred here.

3. Minimize the number of tool-path elements: tool-path elements are a series of line segments representing the travel path of the tool. In general at the ends of tool-path elements, the wire feed rate should be adjusted to avoid deposition error caused by a rapid change of tool-path travel direction. To improve surface accuracy, the number of tool-path elements should be minimized.
4. Simple algorithm with rapid implement: the path planning algorithms should be simple and quick to implement to reduce the pre-processing computational time. Domain decomposition is a frequently used technique in computational geometries that is also useful in AM for path planning [28]. It divides arbitrary layer geometries into a set of simpler shapes, such as monotone polygons or convex polygons, which become easier for path generation. The algorithm for generating zigzag patterns is relatively simple. Therefore domain decomposition of 2D geometries and the filling of the interior area of 2D geometries with zigzag patterns are important to simplify the tool-path generation algorithm.

At this stage, none of the existing path planning algorithm can satisfy all the requirements listed above. Their advantages and disadvantages are summarised in column 3 and 4 of Table 1. Among them, hybrid path planning method meets the requirement 1 and 4, but the number of tool-path passes and tool-path elements should be significantly reduced to suit the WAAM process. A new tool-path planning algorithm, which combines the various advantages of existing methods, is developed to meet this requirement.

3 2D path generation algorithms

A novel tool-path generation strategy that satisfies the requirements of WAAM has been developed. The algorithm firstly decomposes the geometry of each 2D slice into a set of convex polygons. Then for each convex polygon, the outlines are generated with a contour pattern and the interior area is filled with a zigzag pattern. The algorithm for identifying the optimal zigzag direction for a convex polygon has been devised, which can significantly reduce the total number of tool-path elements and hence the number of direction changes. For each sub-polygon, the contour pattern and zigzag pattern are connected to produce one closed curve, reducing the number of tool-path passes. The proposed continuous path generation method is implemented to each sub-polygon independently. Finally, all sub-paths are linked together to form a single continuous path without any starting-stopping sequences for fabricating each 2D slice or layer.

3.1 Decomposition of 2D geometries into convex polygons

STereoLithography (STL) is a commonly used file format for describing the 3D geometry of a component suitable for fabrication using AM. From this format, 2D slices can be readily

generated. The decomposition of these 2D slices into simpler convex polygons, or monotone polygons, will make the implementation of path generation much easier. Many approaches have been developed for decomposing polygons, as described in the survey by Keil [29]. In this research, a divide-and-conquer method is used for decomposing the geometries.

The decomposition method is explained through a flowchart, as shown in Fig.2. After slicing the input 3D CAD model, 2D geometries are obtained. Since STL is a tessellation language, the sliced 2D geometries are a set of polygons.

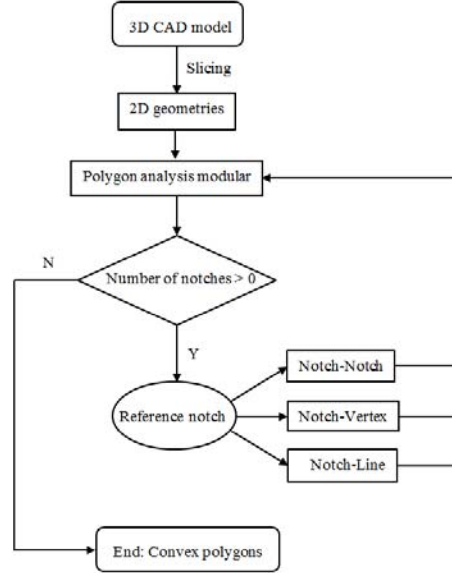


Fig. 2 The flowchart of the developed polygon decomposition method

The polygon analysis modular in Fig.2 consist five steps.

Step 1: Identify the relationships among the polygons. The sliced 2D geometries may contain a number of polygons, either as internally nested shapes or independent entities. Using the concept of “Depth Tree” [18], the depth of a polygon refers to the number of cycles that enclose it. For example, in Fig. 3 (a), there is only one polygon and it has depth of “0”, according to the definition of “Depth Tree”, while in Fig.3 (b) polygon 1 and polygon 2 have depths of “0” and “1”, respectively. Polygons that have even depth numbers are external cycles and those that have odd depth numbers are internal cycles. The details of this method can be found in [30].

Step 2: Order all vertices. In this study, the vertices of external cycles are ordered in clockwise direction, while those vertices of internal cycles are ordered in anti-clockwise direction. As shown in Fig. 3 (a) and (b), all vertices are ordered basing on these rules.

Step 3: Calculate the interior angles of all vertices. Assuming a polygon consists of n vertices, V_1, V_2, \dots, V_n , the interior angle φ_i at V_i can be calculated from Eq.(1) and (2)

$$\sin(\varphi_i) = \frac{\vec{e} \cdot (\overrightarrow{V_i V_{i-1}} \times \overrightarrow{V_i V_{i+1}})}{|\overrightarrow{V_i V_{i-1}}| \cdot |\overrightarrow{V_i V_{i+1}}|}, \quad (1)$$

$$\cos(\varphi_i) = \frac{\overrightarrow{V_i V_{i-1}} \cdot \overrightarrow{V_i V_{i+1}}}{|\overrightarrow{V_i V_{i-1}}| \cdot |\overrightarrow{V_i V_{i+1}}|}. \quad (2)$$

where, φ_i ranges from 0 to 2π and \vec{e} is the unit vector in the buildup direction. Both equations are needed to determine the quadrant of the angle.

Step 4: Identify notches. A notch is defined as a vertex whose interior angle is larger than π . A polygon has at least one notch is called a non-convex polygon; otherwise it is a convex polygon. The process of decomposing a non-convex polygon to convex polygons can be considered to be the process of eliminating notches. For example, the polygon in Fig. 3(a) is a non-convex polygon since the vertices V_2, V_5, V_6 and V_i are notches.

Step 5: Eliminate notches. The next step for polygon decomposition is to eliminate the identified notches. All the notches are sorted by their interior angle. The notch that has the greatest interior angle is set to be the reference notch, which is targeted for elimination. As shown in Fig.4, assuming V_i is the reference notch, two radial lines are generated by extending vectors $\overrightarrow{V_{i-1}V_i}$ and $\overrightarrow{V_{i+1}V_i}$ to intersect with other part of the geometry at points A_i and B_i . There are three different cases along the geometry edges from A_i to B_i . Case 1: there are no vertices between A_i and B_i ; Case 2: there are notches between A_i and B_i ; Case 3: there are vertices between A_i and B_i but none of them are notches.

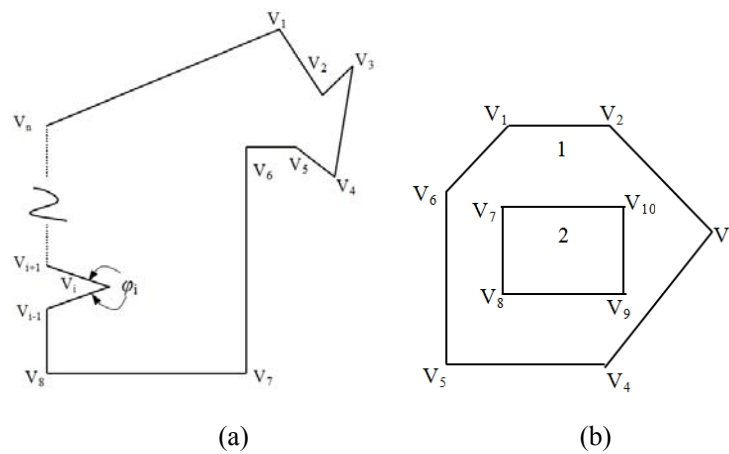


Fig.3 Simple polygon without (a) and with inside island (b)

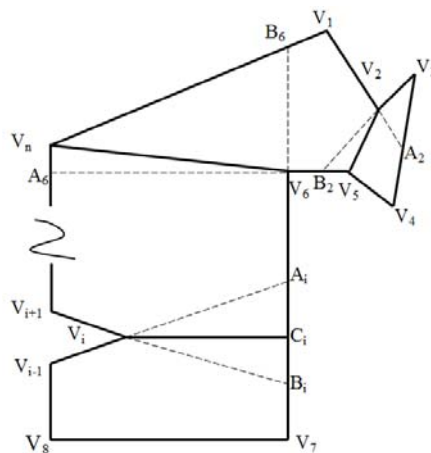


Fig.4 Three different routines for eliminating the reference notch

Three different routines, notch-line decomposition, notch-notch decomposition, and notch-vertex decomposition are used respectively. In notch-line decomposition, “line” means the bisector line of V_i , as shown in Fig.4, V_iC_i is set to be the partitioning line. In notch-notch decomposition, if there is more than one notch, choose the notch that is nearest to the bisector line of V_i as the end point of the partitioning line, or else connect the reference notch and the only existing notch in the scan zone to be the partitioning line, such as V_2V_5 in Fig.4. In notch-vertex decomposition, if there is more than one vertex, choose the vertex that is nearest to the bisector line of V_i as the end point of the partitioning line, or else connect the reference notch and the only existing vertex in the scan zone to be the partitioning line, such as V_6V_n in Fig.4.

The polygon can be decomposed by splitting the notches using only notch-line routines. However, the proposed notch elimination method provides an optimal solution. The notch-notch routine eliminates two notches each time, which will generate a minimal number of convex polygons. The notch-vertex routine generates convex polygons with less edges compared to the notch-line routine, which makes the subsequent steps of path generation more effective.

The flowchart in Fig. 2 shows the recursive use of geometry decomposition modules. The overall decomposition process is terminated when the number of notches in a 2D geometry is equal to zero. The step-by-step process of generating output convex polygons for the simple polygon with an inside island is shown in Fig. 5. This algorithm is able to handle most 2D geometries, except for cases where there are many circular holes inside the geometry. Monotone polygon decomposition would be more suitable in such cases.

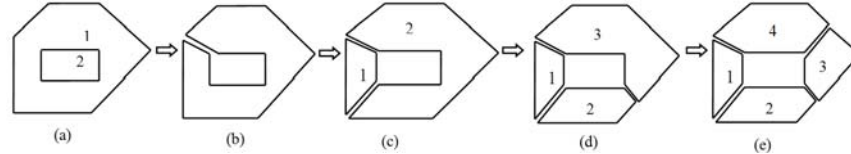


Fig. 5 Step-by-step processes of polygon decomposition

3.2 Path generation for a single convex polygon

For a convex polygon, filling the interior area using a zigzag path is an efficient strategy. To improve the geometrical accuracy, the outline of the convex polygon is fabricated using the contour method. Since a better surface finish can be obtained if there are less welding passes, the interior zigzag pattern and external contour are connected to a continuous path without starting-stopping. In order to minimize the numbers of tool-path elements, an optimal filling direction of zigzag pattern in the convex polygon should be identified. Taking the convex polygon labelled “4” in Fig. 5(e) as an example, the step-by-step algorithm for generating tool-path is described below.

Step 1: Identify the optimal zigzag direction. This problem can be restated as finding the direction where the convex polygon has the minimum height [16]. Lemma 1 explains that the optimal zigzag direction for a convex polygon must be parallel to one of its edges.

Lemma 1. Let P be a convex polygon, and S be an enveloping rectangle for P . For S to have the shortest height, i.e. a minimal number of weld passes is needed to fill S , there must be two vertices of P that lie on one of the long edges of S .

Proof. As shown in Fig.6, a convex polygon P is enclosed with a rectangle S , $ABCD$. Let AB and CD represent the long edges of the enveloping rectangle S . Let H stands for the distance between AB and CD . The problem of finding the optimal inclination of S can be considered to solve the minimum value of H . We assume the vertices V_n and V_m lie on AB and CD respectively. The distance between vertices V_n and V_m has the constant value of L . The angle $\theta_i > 0$, and $\alpha_i > 0$, $i = 1, 2, 3$, and 4. One can obtain the formula,

$$H = L \cdot \sin(\alpha_1 + \theta_1) = L \cdot \sin(\alpha_2 + \theta_2) = L \cdot \sin(\alpha_3 + \theta_3) = L \cdot \sin(\alpha_4 + \theta_4), \quad (3)$$

$$\alpha_1 + \theta_1 = \alpha_3 + \theta_3, \quad (4)$$

$$\alpha_2 + \theta_2 = \alpha_4 + \theta_4, \quad (5)$$

$$\alpha_1 + \theta_1 = \pi - (\alpha_2 + \theta_2). \quad (6)$$

Without discrimination, assume $\alpha_1 + \theta_1 \leq \pi/2$ as shown in Fig. 6, S can be rotated anti-clockwise by $\Delta\theta$, where $0 \leq \Delta\theta \leq \min(\theta_1, \theta_3)$. After rotation, $H = L \cdot \sin(\alpha_1 + \theta_1 - \Delta\theta)$. Since the sine function is a monotonically increasing function in the range from 0 to $\pi/2$, H reaches the minimum value only when $\Delta\theta = \min(\theta_1, \theta_3)$. It demonstrated that H reaches the minimum value as long as one of θ_i is equal to zero by rotating the enveloping rectangle S . Therefore, two vertices of the polygon must lie on one of the long sides of the enveloping rectangle.

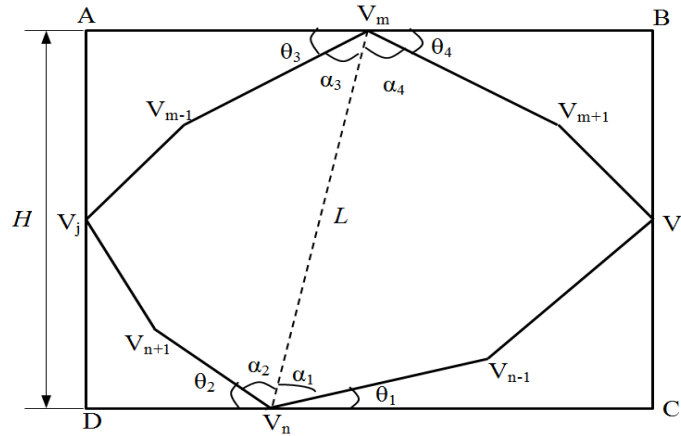


Fig. 6 A case in the proof of Lemma

Lemma 1 indicates that the optimal filling direction must be parallel to one edge of the polygon. Hence, the algorithm for identifying the optimal direction can be described as follows. For each polygon edge, calculate the distance from all the vertices to this edge. As the path should cover all of the polygon area, the maximum value of the distance should be recorded for the referred edge. When the maximum distance for all of the edges have been calculated individually, the edge that has the lowest value is selected as the direction corresponding to the optimal zigzag direction.

Step 2: Determine the left chain. The definition of left chain can be found in [31]. In Fig. 7 (a), EFA is the left chain.

Step 3: Offset the left chain (EFA) and generate a new polygon $A'BCDE'F'A'$.

Step 4: Generate a zigzag pattern with the calculated optimal direction in the interior area of the new polygon.

Step 5: Form a continuous path, as shown in Fig. 7(b).

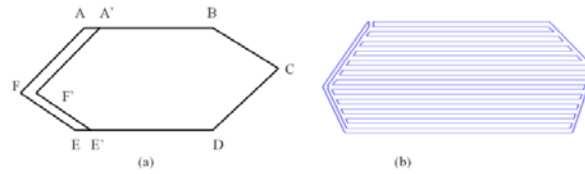


Fig. 7 An example of path generation for a convex polygon

From Step 1 to Step 5, a continuous path with the minimum number of elements can be generated for a convex polygon. Implement this approach independently to all of the convex polygons generated in Fig. 5(e). The completed implementation is shown in Fig. 8(a).

3.3 Path connection

The final step is to connect the sub-paths of each polygon into a closed curve. To improve the surface quality, the connecting points between two polygons are set on the outlines of the geometries.

During the decomposition of 2D geometries, the partition lines were used to regenerate the sub-polygons. The partition lines can be classified into two groups, merging lines and split lines. A merging line merges two polygons into one polygon. As shown in Fig. 5, the step from (a) to (b) is a merging process. A split line separates one polygon into two polygons. In Fig. 5, steps from (b) to (c), (c) to (d) and (d) to (e) are splitting processes. All of the split lines are stored in a new matrix for path connection. Since the split lines separate the polygons, connection lines between the separated polygons are generated that correspond to each of the split lines. As shown in Fig. 8(b), the tool-paths in the area of the circles were reorganized. The proposed method can automatically generate a final closed-looped tool-path as shown in Fig. 8(b). Note that this path planning strategy allows the possibility of connecting paths from consecutive layers of the model to form a continuous space curve in 3 dimensions, spanning multiple layers.

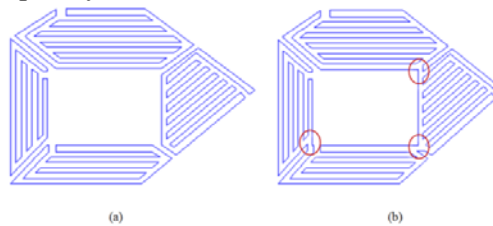


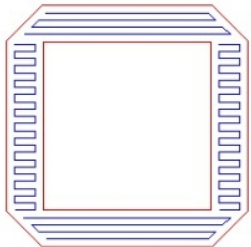
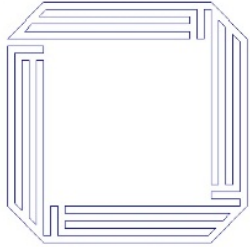
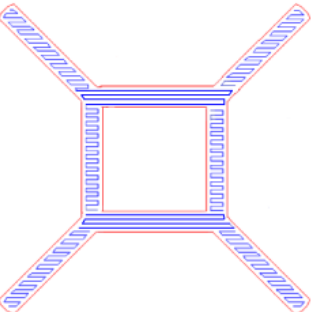
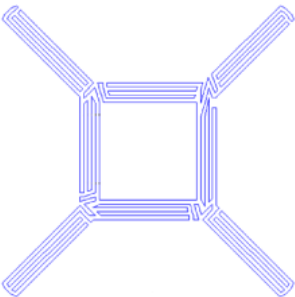
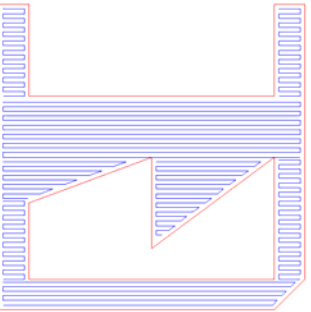
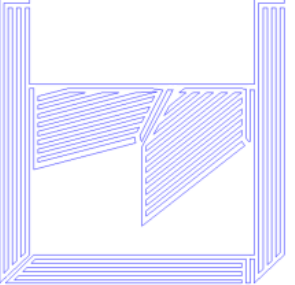
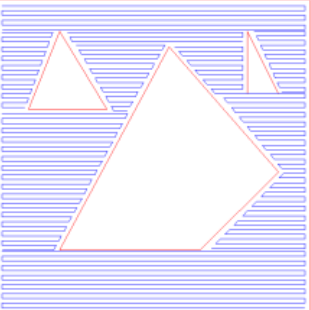

Fig. 8 Final tool-paths connection

4 Implementation and discussion

The performance of the proposed path planning strategy is compared to the existing hybrid method through four sample geometries. The number of tool-path passes and the number of path elements for both methods are summarised in Table 2. The proposed tool-path planning

strategy is capable of generating a continuous tool-path pattern for all examples, while the number of tool-path passes using the hybrid method range from 6 to 11 depending on the complexity of the geometry. Therefore, the surface finish of the part fabricated with the proposed method is expected to be better than hybrid method. In addition, for cases 1, 2 and 3 the number of path elements generated from the proposed method is significantly lower than those produced by the hybrid method. However, for case 4, the number of path elements generated from the proposed method is greater than the hybrid method, indicating that the proposed method is more effective for thin wall structures rather than solid structures.

Table 2. Comparison of the proposed method with the existing hybrid method

No.	Hybrid Method		Proposed Method			
	Tool-path pattern	Passes	Path elements	Tool-path pattern	Passes	Path elements
1		6	120		1	59
2		9	298		1	108
3		10	265		1	191
4		11	291		1	419

Experimental tests were conducted using a robotic welding system at the University of Wollongong. The robotic WAAM system and 3D laser scanning system have been integrated into a welding cell to conduct the experiments, as described in Fig. 9. A computer interface (1) is used to program the experimental processes and collect the experimental results. The robot controller (2) is used to coordinate both the robot motions and welding processes. A programmable GMAW power source (3) is used to control the welding process. A large industrial robot (4) implements the movement of the welding torch (5) for metal deposition, and subsequently a laser profiler (6) to measure the bead profile. An example of weld bead deposits on a work piece is shown (7).

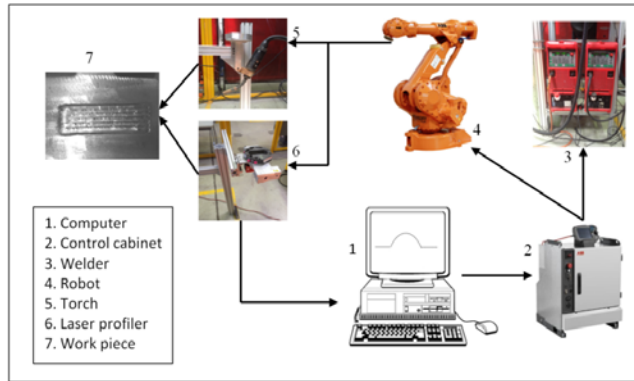


Fig.9 Schematic diagram of the experimental WAAM system

The pulsed-spray GMAW transfer mode was used to minimize the heat input. The wire electrode was mild steel wire with the diameter of 1.2 mm. The stick-out length was set to 20mm to minimise weld spatter for this particular process. A shielding gas mixture of 82% argon and 18% CO₂ was used with a flow rate of 22 L/min. The wire feed rate was set at 5 m/min and the welding speed was 800 mm/min. The first example in Table 2 was used for testing the performance of the proposed method in terms of surface finish, as shown in Fig.10. The surface produced by the proposed method, 10(a), is relatively smoother than that produced by the hybrid method, 10(b). There are some large voids (at Section line 2, 10(b)) resulting from the abrupt stopping of the welding arc on the surface. Additionally, due to the frequent change of path direction in the side zone (at Section line 1, 10(b)), the surface becomes highly uneven, forming ridges that are significantly higher than the edges.

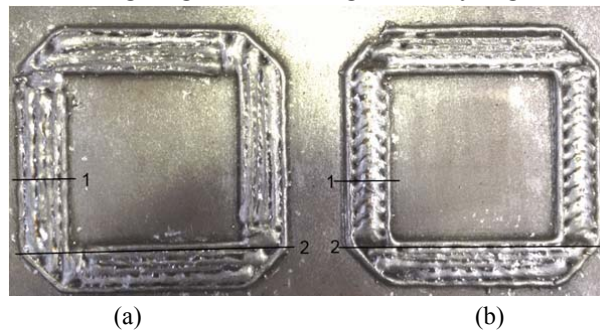


Fig.10 A comparison of the surface finish between the proposed tool-path planning method (a) and the hybrid method (b),

A 3D laser profile scanner with a resolution of 0.02 mm was used to measure the surface profile of the fabricated part. The experimental data obtained from the laser profiler was processed using MATLAB. The measured variations of the surface height along Section lines 1 and 2 (as shown in Fig.10) after the deposition of the third layer are shown in Fig.11. It is found that the height variation for the hybrid method along Section line 1 is significantly larger than that produced by the proposed method, since the proposed path planning strategy produces far fewer changes in direction of travel. Along Section line 2, many voids (zones extremely lower than their surroundings) are formed due to arc starting/stopping effects.

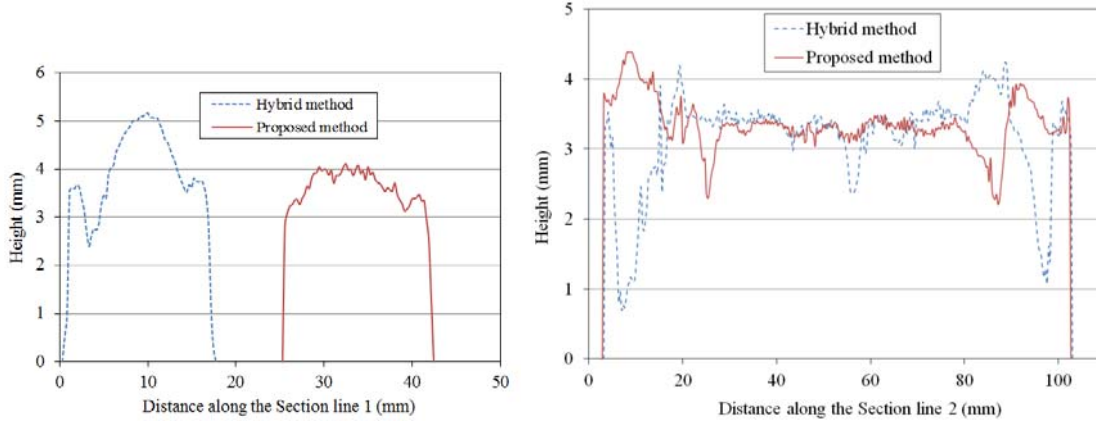


Fig.11 Variation of the heights obtained from the laser profiler

In this test, the comparative measurements of the surface roughness were conducted for three layers. The arithmetic average roughness parameter R_a is calculated, which is defined as

$$R_a = \frac{1}{n} \sum_{i=1}^n |h_i - \bar{h}|, \quad (7)$$

where \bar{h} is the average height of the measured surface, and h_i is the absolute height of each measurement point on the surface. Approximately 100,000 measurement points are used to calculate the surface roughness of each layer and the results are shown in Fig.12. Generally, the surface roughness of the part fabricated using the proposed path planning algorithm is more than 50% lower than that using existing hybrid method. With the increasing deposition of the layers, surface roughness for the proposed method increased slightly, while it was significantly increased for the hybrid method. This is attributable to the design of one continuous tool-path pass and the minimum number of tool-path elements using the proposed method, minimising the effects of starting-stopping and its accumulated deviations over multiple layers.

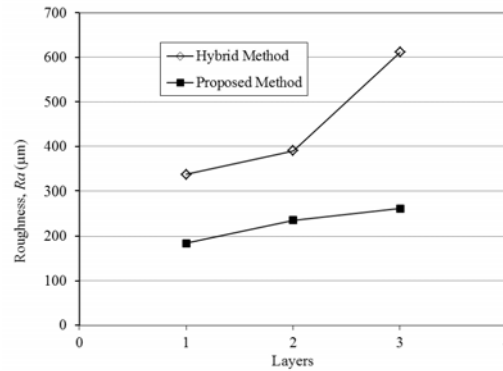


Fig.12 Comparison of the surface roughness between the hybrid method and the proposed method for the first, second and third layers.

Fig.13 shows a comparison of surface variation, including the average, minimum and maximum heights. The average heights of three layers are very similar for both methods. The variation between the maximum value and the minimum value is significantly reduced using the proposed method since arc starting/stopping has a large influence on the surface variation for the hybrid method. After the deposition of three layers, the minimum height of the proposed method is about 3 times higher than that of the hybrid method, indicating that the proposed method is capable of producing a part with higher effective height after surface milling. These preliminary results are very encouraging, and indicate that the proposed tool-path generation strategy is well suited for using WAAM to fabricate complex parts with high surface accuracy.

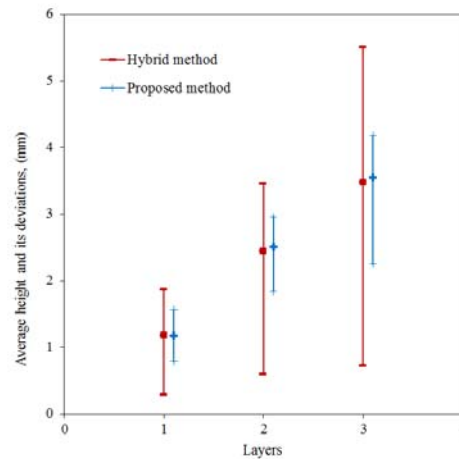


Fig. 13 Comparison of the surface variation between the hybrid method and the proposed method for the first, second and third layers.

5 Conclusions

Tool-path generation is a critical step for a practical WAAM system. A novel tool-path generation strategy has been developed that satisfies the requirements of WAAM. The algorithm firstly decomposes 2D sliced geometry into a set of convex polygons. Then for each convex polygon, the contour pattern and zigzag pattern are implemented and connected to produce one closed curve, reducing the number of tool-path passes. Finally, all sub-paths

are linked together to form a single continuous path without any starting-stopping sequences for fabricating each 2D slice or layer. Both tool-path passes and path elements have been reduced by the proposed method when compared to the existing hybrid method.

The proposed path planning strategy combines the advantages of both zigzag and contour tool-path generation strategies, and its effectiveness have been proven in experimental trials using the WAAM process. The surface roughness and variations of parts fabricated using the proposed path-planning strategy are significantly less than those produced by the existing hybrid method. Further developments toward a mature WAAM system are ongoing, including advanced 3D slicing, distorting mitigation, and post-weld robotic machining processes.

Acknowledgements The authors would like to thank the Defence Materials Technology Centre (DMTC) and the University of Wollongong for providing the research facility. This work is supported in part by the State Scholarship Fund of the China Scholarship Council (No.2011684067).

References

- [1] H. Lipson, "Frontiers in Additive Manufacturing," *Bridge*, vol. 42, pp. 5-12, 2012.
- [2] M. Agarwala, et al., "Direct selective laser sintering of metals," *Rapid Prototyping Journal*, vol. 1, pp. 26-36, 1995.
- [3] G. K. Lewis and E. Schlienger, "Practical considerations and capabilities for laser assisted direct metal deposition," *Materials & Design*, vol. 21, pp. 417-423, 2000.
- [4] K. M. Taminger and R. A. Hafley, "Electron beam freeform fabrication: a rapid metal deposition process," in *Proceedings of the 3rd Annual Automotive Composites Conference*, 2003, pp. 9-10.
- [5] R. Merz, et al., *Shape deposition manufacturing: Engineering Design Research Center*, Carnegie Mellon Univ., 1994.
- [6] P. S. Almeida and S. Williams, "Innovative process model of Ti-6Al-4V additive layer manufacturing using cold metal transfer (CMT)," in *Proceedings of the Twenty-first Annual International Solid Freeform Fabrication Symposium*, University of Texas at Austin, Austin, TX, USA, 2010.
- [7] J. Ding, et al., "Thermo-mechanical analysis of Wire and Arc Additive Layer Manufacturing process on large multi-layer parts," *Computational Materials Science*, vol. 50, pp. 3315-3322, 2011.
- [8] F. Wang, et al., "Morphology investigation on direct current pulsed gas tungsten arc welded additive layer manufactured Ti6Al4V alloy," *The international journal of advanced manufacturing technology*, vol. 57, pp. 597-603, 2011.
- [9] S. Suryakumar, et al., "Weld bead modeling and process optimization in Hybrid Layered Manufacturing," *Computer-Aided Design*, vol. 43, pp. 331-344, 2011.
- [10] F. Martina, et al., "Investigation of the benefits of plasma deposition for the additive layer manufacture of Ti-6Al-4V," *Journal of Materials Processing Technology*, vol. 212, pp. 1377-1386, 2012.
- [11] Y. Zhang, et al., "Weld deposition-based rapid prototyping: a preliminary study," *Journal of Materials Processing Technology*, vol. 135, pp. 347-357, 2003.
- [12] X. Xiong, et al., "Metal direct prototyping by using hybrid plasma deposition and milling," *Journal of Materials Processing Technology*, vol. 209, pp. 124-130, 2009.
- [13] K. Karunakaran, et al., "Low cost integration of additive and subtractive processes for hybrid layered manufacturing," *Robotics and Computer-Integrated Manufacturing*, vol. 26, pp. 490-499, 2010.

- [14] M. R. Dunlavey, "Efficient polygon-filling algorithms for raster displays," *ACM Transactions on Graphics (TOG)*, vol. 2, pp. 264-273, 1983.
- [15] S. C. Park and B. K. Choi, "Tool-path planning for direction-parallel area milling," *Computer-Aided Design*, vol. 32, pp. 17-25, 2000.
- [16] V. Rajan, et al., "The optimal zigzag direction for filling a two-dimensional region," *Rapid Prototyping Journal*, vol. 7, pp. 231-241, 2001.
- [17] R. Farouki, et al., "Path planning with offset curves for layered fabrication processes," *Journal of Manufacturing Systems*, vol. 14, pp. 355-368, 1995.
- [18] Y. Yang, et al., "Equidistant path generation for improving scanning efficiency in layered manufacturing," *Rapid Prototyping Journal*, vol. 8, pp. 30-37, 2002.
- [19] H. Li, et al., "Optimal toolpath pattern identification for single island, sculptured part rough machining using fuzzy pattern analysis," *Computer-Aided Design*, vol. 26, pp. 787-795, 1994.
- [20] H. Wang, et al., "A metric-based approach to two-dimensional (2D) tool-path optimization for high-speed machining," *Transactions-American Society of Mechanical Engineers Journal of Manufacturing Science and Engineering*, vol. 127, p. 33, 2005.
- [21] F. Ren, et al., "Combined reparameterization-based spiral toolpath generation for five-axis sculptured surface machining," *The international journal of advanced manufacturing technology*, vol. 40, pp. 760-768, 2009.
- [22] P. Kulkarni, et al., "A review of process planning techniques in layered manufacturing," *Rapid Prototyping Journal*, vol. 6, pp. 18-35, 2000.
- [23] M. Bertoldi, et al., "Domain decomposition and space filling curves in toolpath planning and generation," in *Proceedings of the 1998 Solid Freeform Fabrication Symposium*, The University of Texas at Austin, Austin, Texas, 1998, pp. 267-74.
- [24] W. Chiu, et al., "Toolpath generation for layer manufacturing of fractal objects," *Rapid Prototyping Journal*, vol. 12, pp. 214-221, 2006.
- [25] T. Wasser, et al., "Implementation and evaluation of novel buildstyles in fused deposition modeling (FDM)," *Strain*, vol. 5, p. 6, 1999.
- [26] R. Dwivedi and R. Kovacevic, "Automated torch path planning using polygon subdivision for solid freeform fabrication based on welding," *Journal of Manufacturing Systems*, vol. 23, pp. 278-291, 2004.
- [27] G. Jin, et al., "An adaptive process planning approach of rapid prototyping and manufacturing," *Robotics and Computer-Integrated Manufacturing*, vol. 29, pp. 23-38, 2013.
- [28] W. Sheng, et al., "Surface partitioning in automated CAD-guided tool planning for additive manufacturing," in *Intelligent Robots and Systems, 2003.(IROS 2003). Proceedings. 2003 IEEE/RSJ International Conference on*, 2003, pp. 2072-2077.
- [29] J. M. Keil, "Polygon decomposition," *Handbook of Computational Geometry*, vol. 2, pp. 491-518, 2000.
- [30] N. Volpato, et al., "Identifying the directions of a set of 2D contours for additive manufacturing process planning," *The international journal of advanced manufacturing technology*, pp. 1-11, 2013.
- [31] M. De Berg, et al., *Computational geometry*: Springer, 2000.